Optimal Siting and Sizing of Energy Storage Systems for Wind Integration

Nhi T. A. Nguyen, Duong D. Le, Cristian Bovo and Alberto Berizzi

***Abstract*—This paper presents an approach to determine the optimal placement and size of ESSs in a high wind penetration grid. Genetic Algorithm (GA) is used to find optimal placement of ESSs so that the combined generation of wind and ESSs is maximized. A cumulant-based multi-period AC Optimal Power Flow (OPF) model with the incorporation of ESSs is developed to take into account wind and load uncertainties in the sizing of the storage devices. The model is tested on IEEE 57-bus system and on real Sicilian system in Italy.**

I. Introduction

Renewable energy has been increasingly integrated into power systems as a result of the effort to reduce CO_2 emissions and build a future power grid economically feasible and environmentally sustainable. Particularly, according to the Blue Map scenario for power supply (IEA, 2008), electricity generation from renewable energy provides a share of 22% of global electricity generation in 2050, which grows almost threefold compared to the Baseline scenario [1]. Along with this growing share of renewable technologies, greater interest has been attracted to the use of Energy Storage Systems (ESSs) due to the variable nature of renewable energy sources. ESSs can accommodate renewable generation in time-shifting its energy to match demand and avoid power curtailment. They can also be used to mitigate transmission congestion and hedge forecast errors, etc.

As wind penetration increases, decision on the size and location of ESSs becomes important for both security of operation and economy of the system. The goal is to place a minimum capacity of ESSs at appropriate sites where their applications will be most exploited. There is a number of studies investigating optimal sizes and sites of ESSs for different applications with wind generation such as compensating short-term wind forecast errors, reducing transmission congestion and minimizing curtailed wind energy. Some papers use deterministic models [2]–[6] while others develop probabilistic approaches to address wind and load uncertainties [7]–[13]. In [7], for example, a stochastic programming methodology is proposed to solve ESS sizing optimization problem in grid-connected wind power plants. The paper takes into account the variability of wind power, system load and electricity prices. The optimization is solved using sample average approximation approach. In [8], chance-constrained programming is employed in optimal sizing of Battery ESS (BESS) for wind power applications. GA combined with Monte-Carlo simulation is used to solve the optimization problem in order to minimize energy cost while keeping the differences between wind/BESS output and a predefined profile within a certain limit. Paper [9] proposes a probabilistic method for sizing an ESS to reduce the effect of uncertainty of short-term wind power forecasts. P. Xiong et al [10] apply a two-stage stochastic model for determining both optimal locations and sizes of ESS under uncertain wind power. A stochastic mixed-integer linear programming formulation is proposed in [11] to co-optimize storage siting and sizing. The approach is applied to a realistic WECC system. References [12] and [13] propose a probabilistic methodology to optimally place ESSs in a deregulated power system. The papers use two-point estimate method to incorporate uncertainties into a DC OPF model. However, the probabilistic DC OPF model with ESS integration is solved independently for each single hour in the whole time frame. This way of solving the model does not adequately represent ESS operation in a deregulated market since the addition of ESSs introduces time inter-dependence behavior into the OPF model. Moreover, computation time is expected to be very high for large-size systems.

In this paper, we propose a combined GA and probabilistic OPF (POPF) model to optimally place and size ESSs in power systems. The ESSs are used for time-shifting wind power to match system demand, hence improve overall system revenue. The GA is applied for optimal siting of the ESSs while the POPF is used for sizing the ESSs under wind and load uncertainties. The POPF is based on cumulant approach, thus can effectively capture system uncertainty into the OPF model. Contribution of the paper includes an approach for optimally place and size ESSs for wind integration, taking into account wind and load uncertainties in the sizing of ESSs. This approach is based on a multi-period AC OPF model, which is a mathematically appropriate approach for studying storage devices, and can be applied for planning problems with ESSs in large systems. The remainder of the paper is organized as follows: In Section II, the POPF model with ESSs is described. Section III describes probabilistic modeling of power injections. In Section IV, the methodology is shown. In section V, tests and results are discussed. Section VI concludes the paper.

II. Probabilistic optimal power flow with ESSs

A. Multi-period AC optimal power flow model

The AC OPF model with ESS integration has the objective function of minimizing ESS capital cost and system total generation cost:

$$\begin{aligned} Min \quad & C_{cap_{ESS}}(B_j^{max}, R_j^{max}) \\ & + \sum_{t=1}^{T}\sum_{i=1}^{ng}[c_{0i} + c_{1i}P_{G,i}^t + c_{2i}(P_{G,i}^t)^2] \\ & + \sum_{t=1}^{T}\sum_{j=1}^{ns}(c_{d,j}P_{d,j}^t - c_{ch,j}P_{ch,j}^t) \end{aligned} \tag{1}$$

where, $C_{cap_{ESS}}(B_j^{max}, R_j^{max})$ is ESS capital cost, which consists of energy-related cost and power-related cost; B_j^{max} and R_j^{max} are respectively energy and power capacity of the ESS at bus *j*; $P_{G,i}^t$ is real generation power at bus *i* in period *t*; $P_{ch,j}^t$ and $P_{d,j}^t$ are charging and discharging power of ESS at bus *j* in period *t*; c_{0i}, c_{1i}, and c_{2i} are cost coefficients of generating unit at bus *i*; $c_{ch,j}$ and $c_{d,j}$ are respectively cost coefficients for charging and discharging power of ESS at bus *j*; *ng* and *ns* are total number of generating units and total number of ESSs, respectively; *T* is the optimization period considered.

The last component in the objective function (1) represents complementary constraints, which make sure the ESS is not charged and discharged at the same time. These constraints are managed by applying suitable fictitious charging and discharging costs (c_{ch} and c_d) for the ESS. When charging, the ESS is treated as a normal load. Therefore, the operational cost of charging is the Locational Marginal Price (LMP) at the ESS bus, and the charging cost c_{ch} is set to zero. To prevent simultaneous charging and discharging, the operational cost of discharging c_d is set to a very small quantity, i.e., c_d = 10^{-2} (\$/MWh), as presented in [14].

This objective function is subject to network constraints and constraints on ESSs.

Power balance equations: Include equations for real and reactive power at each node *i* in each time period *t*:

$$\begin{aligned} & P_{G,i}^t - P_{L,i}^t + P_{d,i}^t - P_{ch,i}^t \\ & = V_i^t \sum_{k=1}^{nb} V_k^t [G_{ik}\cos(\theta_i^t - \theta_k^t) + B_{ik}\sin(\theta_i^t - \theta_k^t)] \end{aligned} \tag{2}$$

$$\begin{aligned} & Q_{G,i}^t - Q_{L,i}^t + Q_{d,i}^t - Q_{ch,i}^t \\ & = V_i^t \sum_{k=1}^{nb} V_k^t [G_{ik}\sin(\theta_i^t - \theta_k^t) - B_{ik}\cos(\theta_i^t - \theta_k^t)] \end{aligned} \tag{3}$$

where, $P_{G,i}^t$ and $Q_{G,i}^t$, $P_{L,i}^t$ and $Q_{L,i}^t$, $P_{d,i}^t$ and $Q_{d,i}^t$, and $P_{ch,i}^t$ and $Q_{ch,i}^t$ are real and reactive generation power of generating unit at bus *i* in period *t*, real and reactive power of load at bus *i* in period *t*, real and reactive discharging power of ESS at bus *i* in period *t* and real and reactive charging power of ESS at bus *i* in period *t*, respectively; V_i^t and V_k^t are voltage magnitude of bus *i* and *k* at period *t*, respectively; θ_i^t and θ_k^t are voltage angle of bus *i* and *k* at period *t*, respectively; G_{ik} and B_{ik} are line conductance and line susceptance of branch *ik*, respectively; nb is the total number of buses in the system.

Upper and lower limits for voltage magnitudes:

$$V_i^{min} \le V_i^t \le V_i^{max} \tag{4}$$

where, V_i^{min} and V_i^{max} are lower and upper limit of voltage magnitude at bus *i*, respectively.

Bounds on real and reactive generation powers:

$$P_{G,i}^{min} \le P_{G,i}^t \le P_{G,i}^{max} \tag{5}$$

$$Q_{G,i}^{min} \le Q_{G,i}^t \le Q_{G,i}^{max} \tag{6}$$

where, $P_{G,i}^{min}$ and $P_{G,i}^{max}$, $Q_{G,i}^{min}$ and $Q_{G,i}^{max}$ are lower and upper limit of real and reactive generation power of generating unit at bus *i*, respectively.

Branch current limits:

$$(I_{ij}^t)^2 \le (I_{ij}^{max})^2 \tag{7}$$

$$(I_{ji}^t)^2 \le (I_{ji}^{max})^2 \tag{8}$$

where, I_{ij}^t and I_{ji}^t are magnitude of the current flowing from bus *i* to bus *j* and from bus *j* to bus *i* in hour *t*, respectively; I_{ij}^{max} and I_{ji}^{max} are upper limit of current flow from bus *i* to bus *j* and from bus *j* to bus *i*, respectively.

ESS energy balance equations:

$$B_i^t = B_i^{t-1} + (\eta_{ch}P_{ch,i}^t - P_{d,i}^t/\eta_d)\Delta t \tag{9}$$

where, B_i^t and B_i^{t-1} are energy of ESS at bus *i* in hour *t* and *t-1*, respectively; $\triangle t$ is the time step.

ESS charging/discharging power bounds:

$$P_{d,i}^{min} \le P_{d,i}^t \le R_i^{max} \tag{10}$$

$$P_{ch,i}^{min} \le P_{ch,i}^t \le R_i^{max} \tag{11}$$

where, $P_{d,i}^{min}$ and $P_{ch,i}^{min}$ are lower limit of real discharging and charging power of ESS at bus *i*.

ESS energy limits:

$$B_i^{min} \le B_i^t \le B_i^{max} \tag{12}$$

where, B_i^{min} is lower limit of energy of ESS at bus *i*.

Budget constraints:

$$\sum_{i=1}^{ns} R_i^{max} \le R^{tot} \tag{13}$$

$$\sum_{i=1}^{ns} B_i^{max} \le B^{tot} \tag{14}$$

where, R^{tot} and B^{tot} are respectively maximum allowable power and energy capacity of the ESSs to be installed.

B. Cumulant-based Probabilistic OPF

Cumulant-based POPF relies on the behavior of random variables ($r.v.$s) when they are combined in a linearized fashion around the solution of a deterministic OPF [15].

When input variables of the OPF problem presented in Section II-A are uncertain, the problem is defined as a POPF problem. The relationship between vectors of output and input $r.v.$s is generally formulated as follows:

$$\boldsymbol{z} = h(\boldsymbol{x}) \tag{15}$$

where, $\boldsymbol{x} = [P^t_{W_i}, P^t_{L_i}]$;
$\boldsymbol{z} = [P^t_{G_i}, P^t_{ch_i}, P^t_{d_i}]$;
$h(\cdot)$: mapping function between input and output.

At the optimum, KKT optimality conditions must be fulfilled [16].

Incorporating wind and load as $r.v.$s into the first-order KKT conditions, we have:

$$F(\boldsymbol{z}, \boldsymbol{x}) = 0 \tag{16}$$

where, $F(\cdot)$ is set of nonlinear equations determining the first-order KKT conditions.

The relationship between $\boldsymbol{z}$ and $\boldsymbol{x}$ is formed by taking full derivative of (16):

$$\mathbf{H}_{\mathcal{L}} \Delta\boldsymbol{z} + \Delta\boldsymbol{x} = 0 \tag{17}$$

where, $\Delta\boldsymbol{z}$ and $\Delta\boldsymbol{x}$ are changes of vectors of output and input $r.v.$s, respectively; $\mathbf{H}_{\mathcal{L}}$ is the Hessian matrix of the Lagrangian function with respect to $\boldsymbol{z}$.

Equation (17) is arranged as:

$$\Delta\boldsymbol{z} = -\mathbf{H}^{-1}_{\mathcal{L}} \Delta\boldsymbol{x} \tag{18}$$

Using linearized relationship (18) and based on the properties of cumulant [17], cumulants of output $r.v.$s can be calculated from cumulants of input $r.v.$s. Probability distributions of output $r.v.$s are then obtained.

III. Probabilistic modeling of power injections

For a power injection in power systems such as load or wind power generation, its stochastic nature can be characterized by a probability density function ($p.d.f.$) and/or a cumulative distribution function ($c.d.f.$). Such functions can be estimated based on historical data. In the literature, load is usually assumed to be characterized by a Gaussian distribution, while wind power generation is usually modeled by various generic continuous distributions such as Gaussian, Beta, Gamma, Weibull, etc.

For wind power, it is hard to fit power output of a wind farm to a common distribution function, since its probability distribution regularity is usually poor. To overcome this issue, a methodology is applied to estimate discrete distributions for wind power output based on measured data: daily wind power profiles of several years are clustered into distinct groups (clusters); daily profiles belonging to each cluster are then used to build each impulse of discrete distribution for each hour; the probability of each impulse (corresponding to each cluster) is calculated proportionally to the total daily profiles; eventually, discrete distribution of wind power output for each hour is obtained. Various techniques have been tested to perform clustering analysis [18]. For the identification of wind power clusters, k-means algorithm is used.

IV. Methodology

The overall methodology of this approach is summarized in the flowchart (Fig. 1). In this approach, optimal location of the ESSs and the expected value of the optimal size are determined by GA and the deterministic OPF. The goal is to minimize ESS investment cost and the total generation cost while maximizing the combined generation of wind and storage. Accordingly, the fitness function is described as:

$$\text{Fitness} = -\frac{\sum\limits_{t=1}^{T}\sum\limits_{i=1}^{nb} P^t_{L_i} - (\sum\limits_{t=1}^{T}\sum\limits_{j=1}^{nw} P^t_{G_j} + \sum\limits_{t=1}^{T}\sum\limits_{k=1}^{ns} P^t_{d_k})}{\sum\limits_{t=1}^{T}\sum\limits_{j=1}^{nw} P^t_{W_j}} \tag{19}$$

GA is an attractive and powerful alternative to other optimization methods in many power system problems because of its robustness and efficiency [19]–[22]. Also, it is appropriate to solve optimal placement problems since traditional derivative-based optimization approaches handle with difficulty the non-convexity, non-linearity and discontinuity of the problem [13]. GA operates based on the mechanics of natural selection and genetics. It starts with a population of randomly generated candidates. Each candidate is called a chromosome and is made by a binary bit string structure that codes, in this paper, the candidate buses for ESSs. Each chromosome has its corresponding fitness which indicates its suitability as an optimal solution. The GA iteratively produces a new population from the old population by means of GA operators. When this cycle of genetic recombination process is iterated for many generations, the overall fitness of the population generally improves [23].

Initially, the first population is randomly generated from the solution space to place the ESSs. The multi-period OPF is run with this placement of the ESSs to minimize the objective function (1). GA, using results from the OPF, evaluates the fitness (19) of each individual in the population. The fitness of individuals is linearly ranked and stochastic universal sampling method is applied to select individuals for breeding. Single point crossover method is applied on the selected individuals to produce new offspring which are then mutated to introduce new genes to the existing solutions. Finally, new offspring are evaluated and reintroduced into the current population to give new population. This routine is repeated until the GA convergence is reached. The best chromosome provides the optimal siting of ESSs, and the optimal solution gives the optimal power capacity R^{max} and energy capacity B^{max} of the ESSs along with their corresponding optimal operational profiles. At this point, optimal locations of ESSs and their capacities are obtained. The probabilistic part of the POPF is performed to assess the risk of not being able to store the available energy during operation of the ESSs due to wind and

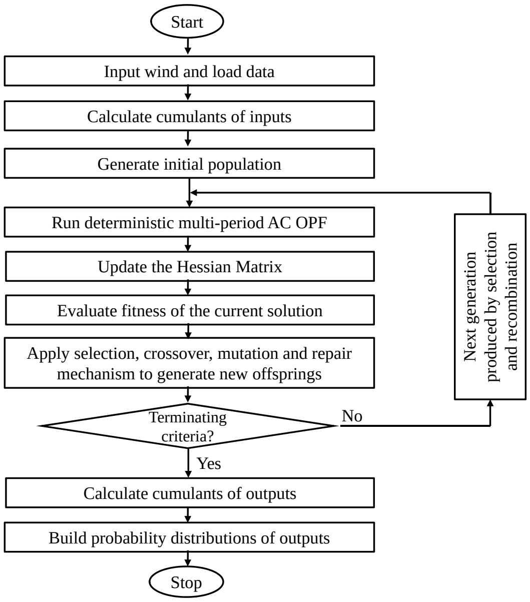

Figure 1. Flowchart of the proposed methodology

load random behavior. Specifically, cumulants of the $r.v.$s at each hour are calculated and probability distributions of ESS capacities are built at each hour. Based on information from these probability distributions, decision makers will finally choose the size of ESSs to be installed.

V. Tests and results

A. IEEE 57-bus system

A test is carried out with the proposed approach on modified IEEE 57-bus system. In this system, total load with a peak of 1620 MW is supplied from both conventional generators and wind. There are 6 conventional generators (at buses 1, 2, 3, 6, 8, and 9) with total capacity of 1565 MW. Wind farms are present in a windy area surrounding bus 12: 450 MW are connected to bus 12 and other smaller wind farms are connected to busses close to bus 12 for a total wind capacity of 750 MW, accounting for 46.3% of wind power penetration. ESSs are to be placed for time-shifting wind energy from off-peak periods (low electricity price) to peak periods (high electricity price) to add economic value to wind energy and avoid wind generation curtailment.

Based on a scale-up version of 3-year measured hourly wind power (from January 1, 2009 to December 31, 2011) of a real wind farm in Sicily, Italy, long-term probability distribution for the total wind power is estimated, using the methodology presented in Section III. Total system load follows the typical daily load profiles of 4 seasons in [24]. Load uncertainty is modeled by assigning it among load buses according to different distributions: loads at buses 15, 38, 44, 50 and 56 are assumed to have Beta distributions with parameters computed by using expected values and standard deviations (assumed to be equal to 10, 12, 9, 8 and 11% of their expected values, respectively) [25]; loads at remaining buses are assumed normally distributed with standard deviations equal to 10% of the expected values.

Result of the combined GA and deterministic OPF is shown in Table I. In this case, the model decided to install 2 ESSs, a bigger one at a wind bus (bus 12) and a smaller one at a load bus (bus 29).

TABLE I. Simulation result of the combined GA and deterministic OPF

Optimal location (Bus number)	B^{max} (MWh)	R^{max} (MW)
12	495.2	95.6
29	172.2	31.0

As an example, operation of the ESS at bus 12 can be seen in Fig. 2. Clearly, the storage is effectively used to time-shift wind energy by charging wind power at low load periods (hours 1 to 7) and then releasing it during the first peak periods of hours 9 to 12 and the second peak periods of hours 20 to 22. There is no wind curtailment and wind power output is fully dispatched.

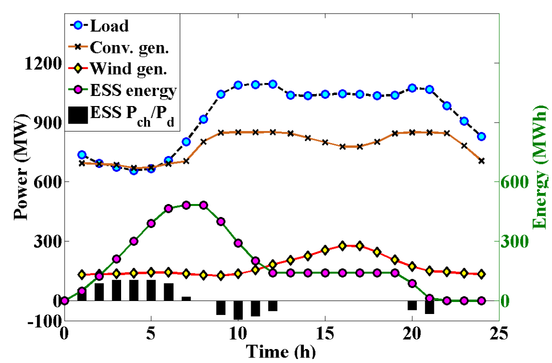

Figure 2. Operation of the ESS at bus 12

Since input variables of the OPF problem are actually stochastic, power and energy capacities of the ESS (i.e., output of the combined GA-OPF problem) are also random variables. Now, the probabilistic assessment is performed on ESS capacities obtained in Table I at the corresponding buses.

According to Fig. 2, the ESS reaches its power capacity (R^{max}) at hours 4 and 5, and reaches its energy capacity (B^{max}) at hour 7, after 6 consecutive charging periods. Since wind and load variation is highest at hour 4, we choose to perform probabilistic assessment for ESS power capacity, based on its operation at this hour. In Fig. 3, we show results of the POPF: $c.d.f.$ of ESS power capacity at hour 4. In this case, installation of the capacity according to Table I would be not enough in some operating conditions. If the decision maker decided to install ESS for a capacity of 143 MW, almost the whole range of the probability distribution would be covered. If a lower value of capacity is decided, it will lead to a risk of not having enough power capacity for handling uncertainty in the system. For example, using 122, 116, 104 and 102 MW will cover 99, 95, 85 and 75% of the whole range of the probability distribution, respectively. This means that if 5% of risk is accepted, for instance, power capacity of the ESS is approximately 18.9% reduced. Similarly, with 15% and 25% of risk allowed, power capacity of the ESS is roughly 27.3% and 28.7% reduced, respectively.

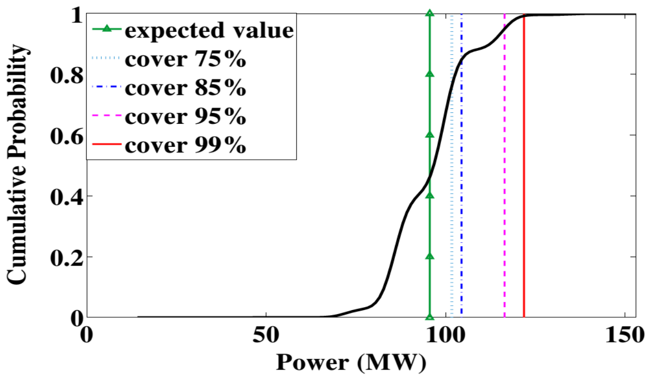

Figure 3. *c.d.f.* of power capacity of ESS at bus 12, hour 4

In Fig. 4, energy capacity of the ESS is probabilistically assessed. As can be noticed from this figure, the use of 708, 627, 592 and 572 MWh will cover 99, 95, 85 and 75% of the whole range of the probability distribution, respectively. This also means that a 5%, 15%, and 25% of risk accepted will result in a reduction of 20.4%, 24.9%, and 27.4% of the energy capacity, respectively.

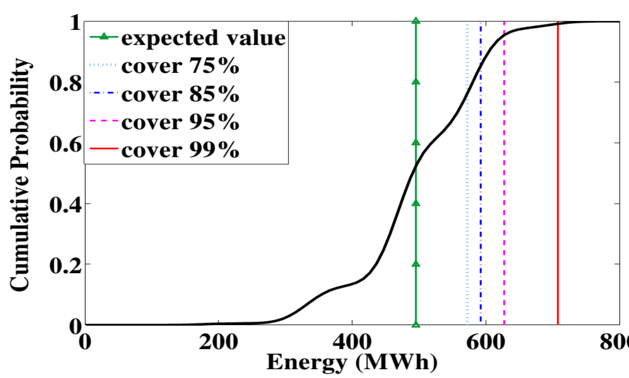

Figure 4. *c.d.f.* of energy capacity of ESS at bus 12, hour 7

In this case, if the decision maker needs to cover 85% of wind and load variations, for instance, power and energy capacity of the ESS at bus 12 has to be 104 MW and 592 MWh, respectively.

B. Sicilian system

Similarly, in this section, the proposed approach is tested on a large network, i.e., Sicilian system. Sicily is the largest island in Italy and Sicilian power system consists of 539 buses, 664 branches and 261 generating units, including 10 wind farms with total installed capacity of 1407 MW. Hourly wind power from September 1, 2011 to August 31, 2012 is used. Total system load with a peak of 5620 MW is assumed to follow the typical daily load profile in Fig. 5. Loads are assumed to have normal distribution with standard deviation of 10% of their expected values.

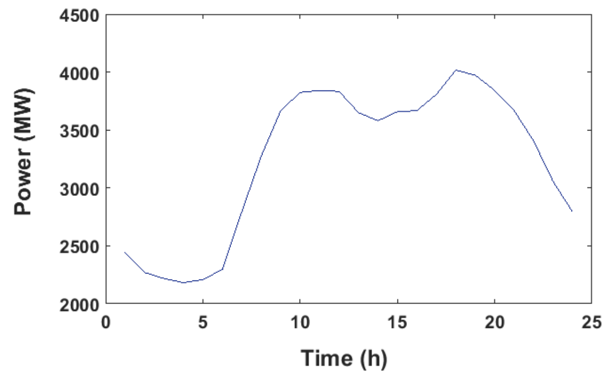

Figure 5. Load profile

Result of the combined GA and deterministic OPF is shown in Table I. In this case, the model decided to install only 1 ESS at a wind bus, i.e., bus 214. This ESS is used to efficiently shift the wind energy from off-peak (hours 1 to 5) to peak periods (hours 10 to 12 and 18 to 20) as shown in Fig. 6.

TABLE II. SIMULATION RESULT OF THE COMBINED GA AND DETERMINISTIC OPF

Optimal location (Bus number)	B^{max} (MWh)	R^{max} (MW)
214	172.0	49.7

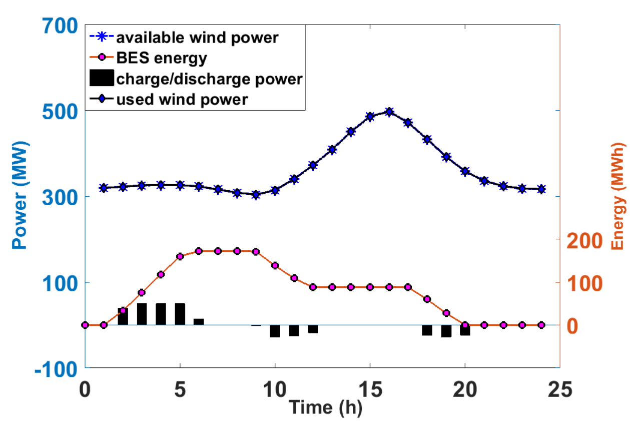

Figure 6. Operation of the ESS

Now, probabilistic assessment is also performed on the obtained ESS capacities in Table II at the corresponding bus: *c.d.f.*s of ESS power and energy capacity are built (figures 7 and 8). Accordingly, in Fig. 7, the use of 49.7 MW (the expected value capacity in Table II) can only cover about 55% of the uncertainty while the use of about 55.9 MW, 58.6 MW, 70.5 MW and 76 MW can cover 75%, 85%, 95% and 99% of the uncertainty, respectively. Likewise, in Fig. 8, the expected value capacity of 172 MW can only handle around 50% of system uncertainty whereas an energy capacity of 211.8 MWh, 222.2 MWh, 240.4 MWh and 282.1 MWh can approximately cover 75%, 85%, 95% and 99% of the uncertainty.

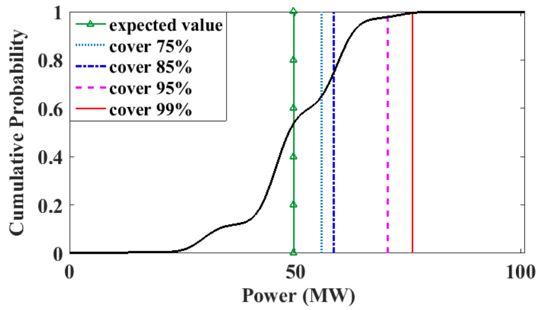

Figure 7. $c.d.f.$ of ESS power capacity, hour 5

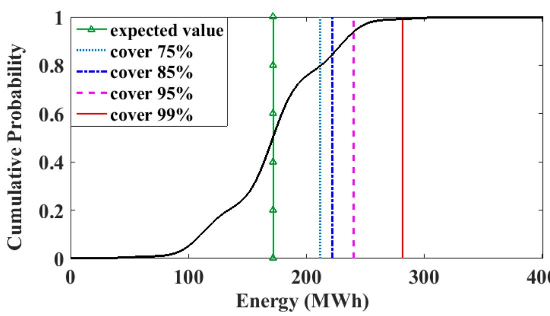

Figure 8. $c.d.f.$ of ESS energy capacity, hour 7

VI. Conclusions

The paper proposes an approach based on the combined GA and probabilistic multi-period AC OPF to optimally place and size ESSs so that the combined generation of ESSs and wind power is maximized. The model effectively captures uncertainty of wind and load resources in the planning of ESSs. The model is extensively tested on IEEE 57-bus system and a real-size system, i.e., Sicilian system. Computing time for the Sicilian system is around 48 hours implemented using Matlab programming language on an Intel core i7 CPU 3.4GHz/8.00 GB RAM PC, which is reasonable for a planning problem. Test results show that to cover higher ranges of uncertainties, ESS capacities are necessarily higher than the expected value capacities. If a certain level of risk is acceptable, both power and energy capacities will be smaller and the model allows to estimate ESS capacities according to the levels of uncertainties to be covered.

References

[1] International Energy Agency, *Energy Technology Perspectives 2010 - Scenarios and Strategies to 2050*, Paris, France, 2010.

[2] W. Z. Chen *et al.*, "Energy Storage Sizing for Dispatchability of Wind Farm," *11^th International Conference on Environment and Electrical Engineering (EEEIC)*, Page(s): 382 - 387, 2012.

[3] Jiajia Song *et al.*, "Optimal placement of energy storage and demand response in the Pacific Northwest," *IEEE Power and Energy Society General Meeting (PES)*, 2013.

[4] Y. M. Atwa, and E. F. El-Saadany, "Optimal Allocation of ESS in Distribution Systems With a High Penetration of Wind Energy," *IEEE Transactions on Power Systems*, vol. 25, no. 4, pp. 1815-1822, Nov. 2010.

[5] P. Fortenbacher, M. Zellner and G. Andersson, "Optimal sizing and placement of distributed storage in low voltage networks," *Power Systems Computation Conference (PSCC)*, Genoa, 2016, pp. 1-7.

[6] N. T. A. Nguyen, D. D. Le, G. G. Moshi, C. Bovo and A. Berizzi, "Sensitivity Analysis on Locations of Energy Storage in Power Systems With Wind Integration," *IEEE Transactions on Industry Applications*, vol. 52, no. 6, pp. 5185-5193, Nov-Dec. 2016.

[7] Z. Shu and P. Jirutitijaroen, "Optimal sizing of energy storage system for wind power plants," *IEEE Power and Energy Society General Meeting*, pp. 1-8, Jul. 2012.

[8] L. Li and L. Yang, "A chance-constrained programming based energy storage system sizing model considering uncertainty of wind power," *International Conference on Sustainable Power Generation and Supply (SUPERGEN)*, pp. 1-6, Sep. 2012.

[9] H. Bludszuweit and J. A. Dominguez-Navarro, "A Probabilistic Method for Energy Storage Sizing Based on Wind Power Forecast Uncertainty," *IEEE Transaction on Power Systems*, Volume: 26, Issue: 3, Page(s): 1651-1658, 2011.

[10] P. Xiong and C. Singh, "Optimal Planning of Storage in Power Systems Integrated With Wind Power Generation," *IEEE Transactions on Sustainable Energy*, vol. 7, no. 1, pp. 232-240, Jan. 2016.

[11] R. Fernandez-Blanco, Y. Dvorkin, B. Xu, Y. Wang and D. S. Kirschen, "Optimal Energy Storage Siting and Sizing: A WECC Case Study," *IEEE Transactions on Sustainable Energy*, vol. 8, no. 2, pp. 733-743, April 2017.

[12] M. Ghofrani, A. Arabali, M. Etezadi-Amoli, and M. Fadali, "A framework for optimal placement of energy storage units within a power system with high wind penetration," *IEEE Transactions on Sustainable Energy*, vol. 4, no. 2, pp. 434-442, Apr. 2013.

[13] M. Ghofrani, A. Arabali, M. Etezadi-Amoli, and M. Fadali, "Energy storage application for performance enhancement of wind integration," *IEEE Trans. Power Syst.*, vol. 28, no. 4, pp. 48034811, Nov. 2013.

[14] A. Castillo, and D. F. Gayme, "Profit maximizing storage allocation in power grids," *Proceedings of the CIGRE*, 2008.

[15] G. Verbic, A. Schellenberg, W. Rosehart, and C. Canizares, "Probabilistic optimal power flow applications to electricity markets," *Probabilistic Methods Applied to Power Systems (PMAPS)*, pp. 1-6, Jun. 2006.

[16] A. Schellenberg, W. Rosehart, and J. Aguado, "Cumulant-Based Probabilistic Optimal Power Flow (P-OPF) With Gaussian and Gamma Distributions," *IEEE Trans. Power Syst.*, vol. 20, no. 2, pp. 773-781, May 2005.

[17] D. D. Le, A. Berizzi, C. Bovo, E. Ciapessoni, D. Cirio, A. Pitto, and G. Gross, "A probabilistic approach to power system security assessment under uncertainty", *Bulk Power System Dynamics and Control - IX Optimization, Security and Control of the Emerging Power Grid, 2013 IREP Symposium*, pp. 1-7, Greece, Aug. 2013.

[18] G. Gan, C. Ma, and J. Wu, *Data Clustering: Theory, Algorithms, and Applications*, Philadelphia, PA: SIAM, 2007.

[19] V. A. Evangelopoulos, and P. S. Georgilakis, "Optimal distributed generation placement under uncertainties based on point estimate method embedded genetic algorithm," *IET Generation, Transmission and Distribution*, vol. 8, no. 3, pp. 389-400, Mar. 2014.

[20] G. Celli, E. Ghiani, S. Mocci, F. Pilo, "A multiobjective evolutionary algorithm for the sizing and siting of distributed generation," IEEE Transaction on Power Systems, vol. 20, no. 2, pp. 750757, 2005.

[21] N. Yang, F. Wen, "A chance constrained programming approach to transmission system expansion planning," Electric Power Systems Research, vol. 75, no. 2-3, pp. 171-177, 2005.

[22] A. G. Bakirtzis, P. N. Biskas, C. E. Zoumas, V. Petridis, "Optimal power flow by enhanced genetic algorithm," IEEE Transaction on Power Systems, vol. 17, no. 2, pp. 229 236, 2002.

[23] T. Numnonda and U. D. Annakkage, "Optimal power dispatch in multinode electricity market using genetic algorithm," *Electric Power Systems Research*, vol. 49, no. 3, pp. 211-220, 1999.

[24] L. Semeraro, E. Crisostomi, A. Franco, A. Landi, M. Raugi, M. Tucci, and G. Giunta, "Electrical load clustering: The Italian case," *Innovative Smart Grid Technologies Conference Europe (ISGT-Europe), 2014 IEEE PES*, Istanbul, pp. 1-6, 12-15 Oct. 2014.

[25] A. Fabbri, T. G. S. Roman, J. R. Abbad, and V. H. M. Quezada, "Assessment of the cost associated with wind generation prediction errors

in a liberalized electricity market," *IEEE Trans. Power Syst.*, vol. 20, no. 3, pp. 1440-1446, Aug. 2005.